Dual-Harmonic Noncontacting Millimeter Waveguide Backshorts: Theory, Design, and Test

MICHAEL K. BREWER AND ANTTI V. RÄISÄNEN

Abstract—**Noncontacting backshorts are necessary in many applications to avoid the wear characteristic of contacting shorts. To reduce losses, it is desirable to eliminate the passband at second harmonic frequencies inherent in conventional quarter-wavelength designs. To this effect, empirically and theoretically designed shorts have been fabricated. The theoretical design extends low-frequency Chebyshev filter theory techniques for use at millimeter-wave frequencies. Both designs have been tested using swept frequency reflectometer techniques. Tests have been carried out over a 40-GHz bandwidth at 100 GHz and a 30-GHz bandwidth at 200 GHz. The results are superior to those obtained with $\lambda/4$ backshorts tested in the same manner.**

I. Introduction

MOVABLE backshorts are needed for RF impedance matching in millimeter-wave devices such as mixers, multipliers, detectors, and oscillators. These devices utilize either a contacting or a noncontacting backshort. Both types suffer from serious problems. Contacting shorts suffer from wear if they are frequently moved. This adversely affects the performance of the device. Noncontacting shorts, on the other hand, suffer from undesired passbands. In particular, the traditional $\lambda/4$ design exhibits a passband at second harmonic frequencies. This can lead to loss due to the active device being resistively terminated at these frequencies.

To avoid these problems, new noncontacting backshort designs have been constructed and tested [1]. The initial motivation for this work was a cooled Schottky diode mixer for use at frequencies between 75 and 120 GHz developed at Five College Radio Astronomy Observatory [2]. The shorts were built for use in quarter-height WR-10 waveguide and were tested at frequencies of 75–116 GHz and 204–232 GHz using frequency swept reflectometer techniques. Parallel to the experimental work, a computer program was developed to enhance the design procedure. This program consists of two parts. The first part uses Chebyshev low-pass filter techniques to design backshorts. The second part plots the theoretical VSWR for shorts that have been designed either empirically or by the first part of the program. Both parts take into account such effects as losses, step discontinuity reactances, and the fact that the guide must be partially filled with dielectric material to prevent contact with the backshort.

Manuscript received April 28, 1981; revised December 4, 1981.

M. K. Brewer is with the Five College Radio Astronomy Observatory, University of Massachusetts, Amherst, MA 01003.

A. V. Räisänen was with the Five College Radio Astronomy Observatory, University of Massachusetts. He is now with Helsinki University of Technology, Radio Laboratory, Otakaari 5A, SF-02150 Espoo, Finland.

II. Design Theory

A. Filter Equations

Matthaei, Young, and Jones [3] describe the use of a lumped element model for the design of low-pass filters for use in coaxial waveguide. This model is also useful for the design of filters in rectangular guide even at millimeter-wave frequencies. Fig. 1(a) shows a typical noncontacting waveguide backshort utilizing alternate low-impedance and high-impedance sections. As shown in Fig. 1(b), both the upper and lower halves of this backshort can be modeled as a series of alternating "pi" and "tee" sections with discontinuity or "fringing" capacitances at each junction. The various inductances and capacitances are further lumped to give the final *LC* filter as shown in Fig. 1(c). The capacitances C_{F0} and C_1 on the terminating end and the inductance l_n on the waveguide end are small and can be ignored without significant effect. Following [3], the elements are assigned g values

$$g_0 = R_0$$
$$g_1, g_3, \cdots, g_{n-1} = \omega_1 L_A, \cdots, \omega_1 L_{N-1}$$
$$g_2, g_4, \cdots, g_n = \omega_1 C_B, \omega_1 C_D, \cdots, \omega_1 C_N$$

where ω_1 is the passband edge of the filter, and R_0 is the terminating impedance of the filter model.

For a Chebyshev response, the g's are calculated as follows:

$$g_0 = 1$$
$$g_1 = 2a_1/\gamma$$
$$g_k = 4a_{k-1}a_k/b_{k-1}g_{k-1}, \qquad k = 2,3,\cdots,n$$
$$\left.\begin{aligned} a_k &= \sin\left[(2k-1)\pi/2n\right] \\ b_k &= \gamma^2 + \sin^2(k\pi/n) \end{aligned}\right\}, \qquad k = 1,2,\cdots,n$$
$$\gamma = \sinh(\beta/2n)$$
$$\beta = \ln\left[\coth\left(R/40\log_{10}e\right)\right]$$

where R is the desired passband ripple in decibels, and n is the total number of sections in the filter. All values are

0018-9480/82/0500-0708$00.75

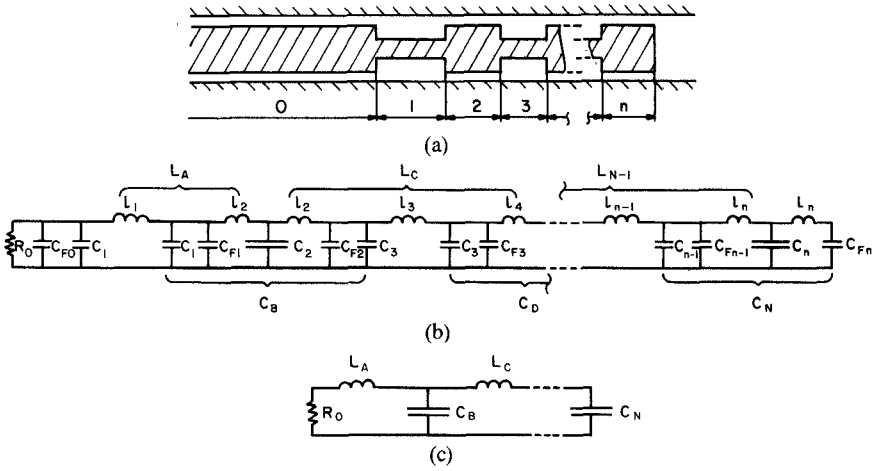

Fig. 1. (a) Alternating high-low impedance noncontacting backshort. (b) Quasi-lumped circuit. (c) Lumped circuit.

normalized to $g_0 = 1$. The lumped reactances of the individual sections are then given by

$$\begin{aligned}
\omega_1 L_A &= R_0 g_1 = \omega_1 l_1 + \omega_1 l_2 \\
&= Z_{C1}\sin(\beta_1 z_1) + Z_{C2}\tan(\beta_2 z_2/2) \\
\omega_1 L_C &= R_0 g_3 = \omega_1 l_2 + \omega_1 l_3 + \omega_1 l_4 \\
&= Z_{C2}\tan(\beta_2 z_2/2) + Z_{C3}\sin(\beta_3 z_3) \\
&\quad + Z_{C4}\tan(\beta_4 z_4/2) \\
&\vdots \\
\omega_1 L_{N-1} &= R_0 g_{n-1} = \omega_1 l_{n-2} + \omega_1 l_{n-1} + \omega_1 l_n \\
&= Z_{Cn-2}\tan(\beta_{n-2} z_{n-2}/2) \\
&\quad + Z_{Cn-1}\sin(\beta_{n-1} z_{n-1}) \\
&\quad + Z_{Cn}\tan(\beta_n z_n/2) \qquad \text{(1a)}
\end{aligned}$$

and

$$\begin{aligned}
\omega_1 C_B &= g_2/R_0 = \omega_1 C_1 + \omega_1 C_{F1} + \omega_1 C_2 + \omega_1 C_{F2} + \omega_1 C_3 \\
&= Y_{C1}\tan(\beta_1 z_1/2) + \omega_1 C_{F1} + Y_{C2}\sin(\beta_2 z_2) + \omega_1 C_{F2} \\
&\quad + Y_{C3}\tan(\beta_3 z_3/2) \\
&\vdots \\
\omega_1 C_{N-2} &= g_{n-2}/R_0 = \omega_1 C_{n-3} + \omega_1 C_{Fn-3} + \omega_1 C_{n-2} \\
&\quad + \omega_1 C_{Fn-2} + \omega_1 C_{n-1} \\
&= Y_{Cn-3}\tan(\beta_{n-3} z_{n-3}/2) + \omega_1 C_{Fn-3} \\
&\quad + Y_{Cn-2}\sin(\beta_{n-2} z_{n-2}) \\
&\quad + \omega_1 C_{Fn-2} + Y_{Cn-1}\tan(\beta_{n-1} z_{n-1}/2) \\
\omega_1 C_N &= g_n/R_0 = \omega_1 C_{n-1} + \omega_1 C_{Fn-1} + \omega_1 C_n + \omega_1 C_{Fn} \\
&= Y_{Cn-1}\tan(\beta_{n-1} z_{n-1}/2) + \omega_1 C_{Fn-1} \\
&\quad + Y_{Cn}\sin(\beta_n z_n) + \omega_1 C_{Fn} \qquad \text{(1b)}
\end{aligned}$$

where z_i is the length of section i, and $Z_{Ci}(Y_{ci})$ is the characteristic impedance (admittance) of section i.

The lengths of the individual sections are found by employing an iterative technique. On the first iteration the relatively small tangent terms in (1) are ignored, and the equations for the z_i are solved directly. Succeeding iterations then substitute the z_{i-1} and z_{i+1} from the previous iteration into the tangent terms and again solve directly for the z_i. This process is continued until convergence is obtained. Typically, this takes about five iterations.

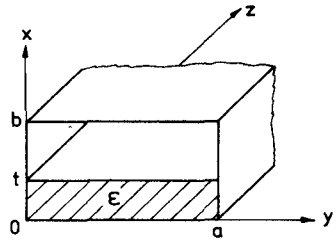

Fig. 2. Partially dielectric-filled rectangular waveguide.

B. Characteristic Impedances

In order to insure that the backshort does not contact the top and bottom of the waveguide, a thin strip of dielectric material is folded over it before insertion into the guide. As a result, each section of the backshort must be modeled as a waveguide partially filled with dielectric material. As shown in Fig. 2, the guide consists of two regions. The first, between 0 and t, contains material with relative dielectric constant ϵ while the second, between t and b, is filled with air. As discussed by Harrington [4], the fields which satisfy the boundary conditions at the walls of the guide are

$$\begin{aligned}
\psi_d &= C_d \cos(k_{xd} x)\sin(n\pi y/a) e^{-j\beta z} \\
\psi_a &= C_a \cosh\left[k_{xa}(b-x)\right]\sin(n\pi y/a) e^{-j\beta z}
\end{aligned}$$

where

$$\begin{aligned}
k_{xa} &= \left[\beta^2 - k_0^2 + (n\pi/a)^2\right]^{1/2} \\
k_{xd} &= \left[k_0^2\epsilon - \beta^2 - (n\pi/a)^2\right]^{1/2} \\
k_0 &= 2\pi/\lambda_0. \qquad \text{(2)}
\end{aligned}$$

These formulas have been modified from those given in [4] to make k_{xa} a real quantity.

The dominant mode in this situation is the LSM_{11} mode ([5]). For this mode we have the equations

$$E_x = 1/j\omega\epsilon \times (\partial^2/\partial x^2 + k_0^2\epsilon)\psi, \qquad H_x = 0$$
$$E_y = 1/j\omega\epsilon \times \partial^2\psi/\partial x\,\partial y, \qquad H_y = \partial\psi/\partial z$$
$$E_z = 1/j\omega\epsilon \times \partial^2\psi/\partial x\,\partial z, \qquad H_z = -\partial\psi/\partial y.$$

These yield for the fields in the dielectric

$$E_{xd} = 1/j\omega\epsilon \times (k_0^2\epsilon - k_{xd}^2) \times C_d \cos(k_{xd}x)\sin(\pi y/a)e^{-j\beta z}$$
$$E_{yd} = -1/j\omega\epsilon \times k_{xd}\pi/a \times C_d \sin(k_{xd}x)\cos(\pi y/a)e^{-j\beta z}$$
$$E_{zd} = 1/\omega\epsilon \times k_{xd}\beta \times C_d \sin(k_{xd}x)\sin(\pi y/a)e^{-j\beta z}$$
$$H_{yd} = -j\beta \times C_d \cos(k_{xd}x)\sin(\pi y/a)e^{-j\beta z}$$
$$H_{zd} = -\pi/a \times C_d \cos(k_{xd}x)\cos(\pi y/a)e^{-j\beta z}.$$

While for the fields in air we have

$$E_{xa} = 1/j\omega \times (k_0^2 + k_{xa}^2) \times C_a \cosh[k_{xa}(b-x)]\sin(\pi y/a)e^{-j\beta z}$$
$$E_{ya} = -1/j\omega \times k_{xa}\pi/a \times C_a \sinh[k_{xa}(b-x)]\cos(\pi y/a)e^{-j\beta z}$$
$$E_{za} = 1/\omega \times k_{xa}\beta \times C_a \sinh[k_{xa}(b-x)]\sin(\pi y/a)e^{-j\beta z}$$
$$H_{ya} = -j\beta \times C_a \cosh[k_{xa}(b-x)]\sin(\pi y/a)e^{-j\beta z}$$
$$H_{za} = -\pi/a \times C_a \cosh[k_{xa}(b-x)]\cos(\pi y/a)e^{-j\beta z}.$$

Continuity of E_y and E_z gives

$$k_{xd}C_d \sin(k_{xd}t) = \epsilon k_{xa}C_a \sinh[k_{xa}(b-t)].$$

Continuity of H_y and H_z gives

$$C_d \cos(k_{xd}t) = C_a \cosh[k_{xa}(b-t)].$$

Thus, we have the dispersion relation

$$k_{xd}\tan(k_{xd}t) = \epsilon k_{xa}\tanh[k_{xa}(b-t)]. \tag{3}$$

The unknown β^2 is calculated by first assuming that k_{xa} and k_{xd} are quite small; thus, (3) becomes approximately

$$k_{xd}^2 t \cong \epsilon k_{xa}^2 (b-t).$$

Equation (2) gives

$$k_{xa}^2 = k_0^2(\epsilon - 1) - k_{xd}^2. \tag{4}$$

So we have the approximate equation

$$k_{xd}^2 \cong k_0^2(\epsilon - 1)\epsilon(b-t)/[\epsilon(b-t) + t].$$

Using (3) and (4), we then form the objective function

$$F(k_{xd}) = k_{xd}\tan(k_{xd}t) - \epsilon k_{xa}\tanh[k_{xa}(b-t)]$$

and its derivative

$$F'(k_{xd}) = \tan(k_{xd}t) + k_{xd}t \times \sec^2(k_{xd}t) + \epsilon k_{xd}/k_{xa} \times \tanh[k_{xa}(b-t)] + \epsilon k_{xd}(b-t) \times \operatorname{sech}^2[k_{xa}(b-t)]$$

where we have used the fact that $k'_{xa} = -k_{xd}/k_{xa}$. The exact numerical value for k_{xd} is then found by using Newton's method modified so that the solution lies between 0 and the first pole of $\tan(k_{xd}t)$. Substitution into (2) then gives β as desired.

The characteristic impedance, for the dominant mode, of each section is then given by

$$Z_{Ci} = 2Z_0 b_i k_0/a\beta_i, \qquad i = 1, 2, \cdots, n$$

where $Z_0 = 376.6\ \Omega$.

C. Discontinuity Capacitances

The discontinuity capacitances are modeled as lumped capacitive elements located at the discontinuities. The formula for these capacitances is given by Marcuvitz [6]. With α as the ratio of the height of the low-impedance section to that of the high-impedance section, and Z_c and λ_g as calculated for the high-impedance section

$$B_F = 4b/Z_C\lambda_g \times (\eta + 2/\xi)$$

where

$$\eta = \ln[(1-\alpha^2)/4\alpha] + 1/2 \times (\alpha + 1/\alpha) \times \ln[(1+\alpha)/(1-\alpha)]$$

and

$$\xi = [(1+\alpha)/(1-\alpha)]^{2\alpha} \times \left\{1 + \left[1 - (2b/\lambda_g)^2\right]^{1/2}\right\} / \left\{1 - \left[1 + (2b/\lambda g)^2\right]^{1/2}\right\} - (1+3\alpha^2)/(1-\alpha^2).$$

Using this formula is equivalent to making the approximation that the high-impedance section is completely filled with a dielectric whose constant gives β as calculated. Accuracy may be somewhat impaired by the discontinuous dielectric constant actually present. These capacitances are, however, a small effect.

D. Losses

In order to calculate the final VSWR of the short we take into account losses in the guide walls and dielectric material.

The total power flowing in the guide is the sum of that flowing in the dielectric portion and that flowing in the air portion. Thus

$$\begin{aligned} P_{\text{tot}} &= 1/2 \times \int_0^a \int_0^t E_{xd}H_{yd}^* dx\,dy + 1/2 \times \int_0^a \int_t^b E_{xa}H_{ya}^* dx\,dy \\ &= \beta/2\omega\epsilon \times (k_0^2\epsilon - k_{xd}^2) \times C_d^2 \int_0^a \int_0^t \cos^2(k_{xd}x)\sin^2(\pi y/a)\,dx\,dy \\ &\quad + \beta/2\omega \times (k_0^2 + k_{xa}^2) \times C_a^2 \int_0^a \int_t^b \cosh^2[k_{xa}(b-x)]\sin^2(\pi y/a)\,dx\,dy \\ &= \beta a/8\omega \times [\beta^2 + (\pi/a)^2] \times C_d^2 \times \{1/\epsilon \times [t + \sin(2k_{xd}t)/2k_{xd}] \\ &\quad + \cos^2(k_{xd}t)/\cosh^2[k_{xa}(b-t)] \\ &\quad \times [(b-t) + \sinh(2k_{xa}(b-t))/2k_{xa}]\}. \end{aligned}$$

The power dissipated in the dielectric is given by

$$P_d = \omega\epsilon''/2 \times \int_0^a \int_0^t |E_{xd}|^2 dx\, dy$$
$$= \epsilon''/2\epsilon^2\omega \times (k_0^2\epsilon - k_{xd}^2) \times C_d^2 \int_0^a \int_0^t \cos^2(k_{xd}x)\sin^2(\pi y/a)\, dx\, dy$$
$$= \epsilon'' a/8\epsilon^2\omega \times (k_0^2\epsilon - k_{xd}^2) \times C_d^2 [t + \sin(2k_{xd}t)/2k_{xd}].$$

That dissipated in the guide walls is given by

$$P_g = R_s/2 \times \left\{ \int_0^a [|H_{yd}(x=0)|^2 + |H_{zd}(x=0)|^2 + |H_{ya}(x=b)|^2 + |H_{za}(x=b)|^2]\, dy + \int_0^t [|H_{zd}(y=0)|^2 + |H_{zd}(y=a)|^2]\, dx + \int_t^b [|H_{za}(y=0)|^2 + |H_{za}(y=a)|^2]\, dx \right\}$$

where $R_s = (k_0 Z_0/2\sigma)^{\frac{1}{2}}$. Thus

$$P_g = R_s/2 \times C_d^2 \left\{ [1+\cos^2(k_{xd}t)/\cosh^2(k_{xa}(b-t))] \times \int_0^a [\beta^2 \sin^2(\pi y/a) + (\pi/a)^2 \cos^2(\pi y/a)]\, dy + 2(\pi/a)^2 \left[\int_0^t \cos^2(k_{xd}x)\, dx + \cos^2(k_{xd}t)/\cosh^2(k_{xa}(b-t)) \times \int_t^b \cosh^2(k_{xa}(b-x))\, dx \right] \right\}$$
$$= R_s/4 \times C_d^2 \{ [1+\cos^2(k_{xd}t)/\cosh^2(k_{xa}(b-t))] \times [\beta^2 a + \pi^2/a] + 2(\pi/a)^2 \times [t + \sin(2k_{xd}t)/2k_{xd} + \cos^2(k_{xd}t)/\cosh^2(k_{xa}(b-t)) \times \{(b-t) + \sinh(2k_{xa}(b-t))/2k_{xa}\}] \}.$$

The required loss coefficient α is then given by

$$\alpha = (P_d + P_g)/2P_{\text{tot}}.$$

E. VSWR Calculations

The final VSWR of the model is obtained by translating the impedance of the zeroth section through the filter using standard formulas and adding the fringing reactance at each junction. Thus

$$Y_l = Y_{Cl} \times [Y_{l-1} + Y_{Cl}\,\text{ctanh}(\gamma l_l)]/[Y_{Cl} + Y_{l-1}\,\text{ctanh}(\gamma l_l)] + jB_{Fl}$$

where ctanh is the complex hyperbolic tangent and $\gamma = \alpha + j\beta$.

The VSWR is calculated comparing the final impedance with half of the guide impedance. This because the model computes the upper half of the backshort and assumes that the lower half is symmetric.

III. Numerical Techniques

A. Computer Program

A versatile interactive computer program was developed making it possible not only to design backshorts using the above filter theory or enter entire empirical designs, but also to examine the effects of such modifications as scaling the lengths of the sections with frequency or adjusting one or more sections individually. The program then uses standard DIGRAPH [7] subroutines to plot such things as VSWR, return loss, and impedance on the screen of a Tektronics 4010 graphics terminal. The entire process of design and plot of one backshort design takes less than one second of CPU time on a CDC CYBER 175 system and typically less than one minute of real time. In this manner, many designs can be examined quite quickly, and the effects of modifications on the designs can be empirically understood.

B. Design Techniques

A good backshort should have a very low input impedance compared to the guide impedance over the entire bandwidth of interest. Thus, since the model used here is that of a low-pass filter, there are three requirements on its attenuation curve. First, the passband edge should be as low in frequency as possible. Second, the slope of the attenuation curve should be as steep as possible. And, third, the stopband region should be as wide as possible.

In order to attain these goals, there are several parameters that can be adjusted. In the following, these parameters and the constraints on and effects of their adjustment will be discussed.

1) Section Lengths: The lengths of the individual sections are the most important factor in determining the filter characteristics. If the section lengths are too short, the filter will never attain a very high VSWR and will tend to be totally ineffective at the lower end of the frequency band. On the other hand, if the lengths are allowed to approach half-wave resonance they will create holes in the stopband. In general, the section lengths should lie between $\lambda_g/8$ and $3\lambda_g/8$. This is cyclic in that lengths between $5\lambda_g/8$ and $7\lambda_g/8$, etc., are also acceptable. Note, however, that longer section lengths also incur greater losses which will adversely affect the attenuation characteristics of the filter.

2) Section Heights: In order to minimize the lengths of the sections, it is desirable to make the ratio of the heights of the high- and low-impedance sections as great as possible. In practice, these are constrained by mechanical rigidity in the case of the high-impedance sections, and by the requirement that there be a dielectric-filled gap in that of the low-impedance sections.

3) Model Terminating Impedance: The zeroth section terminating impedance of the filter model is constrained to

lie between that of the high-impedance sections and that of the low-impedance sections. It should be set as low as possible to create a large mismatch to the guide impedance near the passband edge. If it is set too low, however, the required impedance ratios of the design will force the low-impedance sections to approach half-wave resonance. Specifically, lowering the terminating impedance lengthens the low-impedance sections while shortening the high-impedance sections. Raising the terminating impedance has the opposite effect. This impedance is an artifact of the model in that setting it equal to that of the low-impedance sections after the filter is computed has very little effect on the attenuation characteristics of the resultant backshort. This has been done with the backshorts that have been constructed to enhance their rigidity.

4) Model Passband Edge: The passband edge of the model should be made as low in frequency as possible to maximize the usefulness of the short at the lower end of the waveguide band. On the other hand, the filter model is based upon the guide impedances calculated at this frequency. Thus, if the passband edge is set too near the cutoff frequency of the waveguide, the divergent guide impedances will be far from those present in the guide at higher frequencies. It would then seem that the attenuation characteristics of the resultant filter model would be adversely affected. In practice however, because of considerations to be discussed below, it is possible to set the passband edge very near the guide cutoff frequency.

5) Design Passband Ripple: Though we are not interested in the passband of the model, the design passband ripple affects the slope of the attenuation curve and the overall width of the stopband. Increasing the ripple results in a steeper slope and a narrower stopband. Thus, this parameter is quite important in adjusting the stopband to cover the region of interest.

6) Number of Filter Sections: As the number of sections increases, the slope and height of the attenuation curve increases. The required impedance ratios of the sections also increase, however, so the individual sections are forced to become longer, thus decreasing the stopband width. Waveguide losses, also, become important for longer shorts so a point of diminishing returns is rapidly reached. We have found that five sections seem to be about the optimum number for maximum slope, VSWR, and stopband width.

7) Other Considerations: One other consideration in backshort design is the variation of guide impedances and discontinuity capacitances with frequency. As it turns out, these variations do not damage the attenuation characteristics of the model shorts. For the inductances, the characteristic guide impedance decreases with increasing frequency partially offsetting the increase in the sine and tangent factors in (1). For the capacitances, the opposite is true. The increasing characteristic admittances enhance the increase in the sine and tangent factors. This tendency is somewhat offset by the fact that the discontinuity capacitances are proportional to λ_g. Thus they decrease with increasing frequency. It has been found that this offsetting can be further enhanced by using in (1) capacitances calculated at a higher frequency than ω_1. All combined, these factors actually somewhat increase the width of the stopband region for the model shorts. They also account for the fact that the bandpass edge can be set very close to the guide cutoff frequency which at first seems to be contraindicated.

TABLE I
SECTION LENGTHS FOR TEST BACKSHORTS (mm)

Design	SECTION 1	2	3	4
Chebyhev	0.46	0.24	1.12	0.24
Empirical	0.86	0.44	0.51	0.65
λ/4	0.91	0.56	0.84	0.51

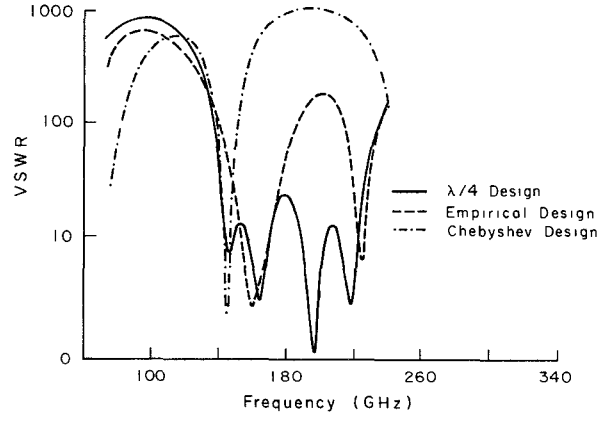

Fig. 3. Theoretical VSWR curves.

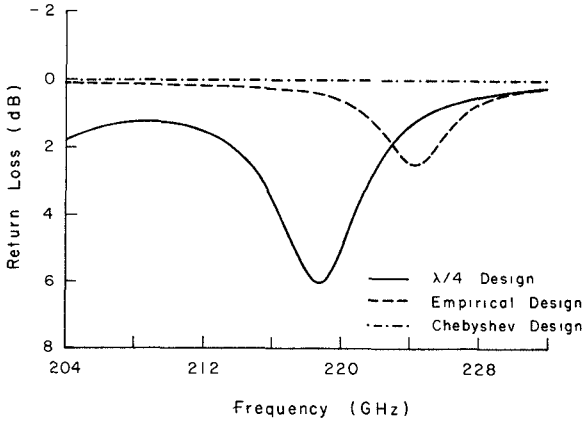

Fig. 4. Theoretical return loss at second harmonic frequencies.

C. Design Results

Three backshort models were chosen for construction. The section lengths for these backshorts are given in Table I. All were five-section filters. The assumed conductivity of the shorts and guide walls was 0.60 times that of smooth copper ([8]). The relative dielectric constant of the insulating mylar was taken to be 3.06 with a loss tangent of 0.001.

The first model was derived from the Chebyshev low-pass

filter theory. As shown in Fig. 3, its response is characterized by a very smooth stopband with quite sharp edges. While it was not found possible to attain a single stopband which covered both the fundamental and harmonic bands, it was discovered that through lengthening one section until it became half-wave resonant between the two bands of interest the stopband could be extended to cover the entire second harmonic region.

The second model was an empirical design approached by using experience concerning backshorts and RF chokes gained through earlier millimeter-wave mixer work (e.g., [9]). While its theoretical response (Figs. 3 and 4) is not as well behaved as that of the Chebyshev derived design, it still attains an adequate VSWR in the second harmonic band.

The third model short was a conventional $\lambda/4$ design which was constructed for purposes of comparison with the two previous designs. As can be seen in Figs. 3 and 4, its theoretical response is considerably worse in the 150–240-GHz region than either of the other two shorts. This was borne out by experiment.

IV. Experimental Techniques

A. Backshort Construction

In the cooled mixer [2], the waveguide (WR-10) channel is reduced to one-quarter height having dimensions 2.54 mm×0.30 mm. To fit into this guide, the backshorts were made of 0.25-mm-thick copper plated brass and insulated from the waveguide by 19-μm-thick mylar tape. Reasons for using brass are its strength and easy machinability. A copper plating about 1-μm thick was applied to improve the surface conductivity. This procedure was found to be important. Gold plating was also tried but it was much more difficult and produced worse results than copper. The general structure of the backshorts is shown in Fig. 5.

B. Measurement Setup

The backshorts were tested in a test waveguide similar to the waveguide channel in the cooled mixer mentioned above. The test waveguide was also made of copper plated brass. The transition from full height WR-10 waveguide to one-quarter height was made by a linear taper 23 mm long. The waveguide block consists of two pieces, one containing the waveguide channel and the other consisting of a flat mating surface. The contacting edges make an acute angle to insure good electrical contact. The loss of the test guide taper has been measured to be 0.2–0.4 dB at 75–116 GHz.

Reflectometer techniques were used to test the backshorts. A thin sheet of copper pressed between the directional coupler and the test waveguide was used as a reference short. The backshorts were tested at both 75–116 GHz and 204–232 GHz. Fig. 6 shows the experimental setup at the second harmonic band. The output of a frequency swept BWO was doubled using a Schottky diode frequency multiplier ([10]) which provided an output power of 1–5 mW over the 204–232-GHz band. At both frequency bands directional couplers of 20-dB coupling and 40-dB

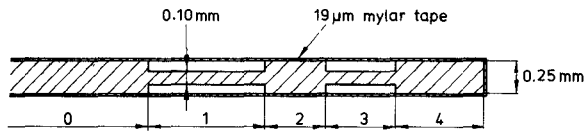

Fig. 5. Test backshort structure.

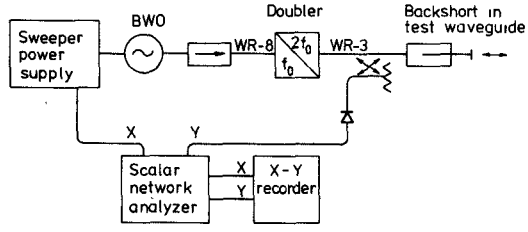

Fig. 6. Measurement setup for frequencies over 200 GHz.

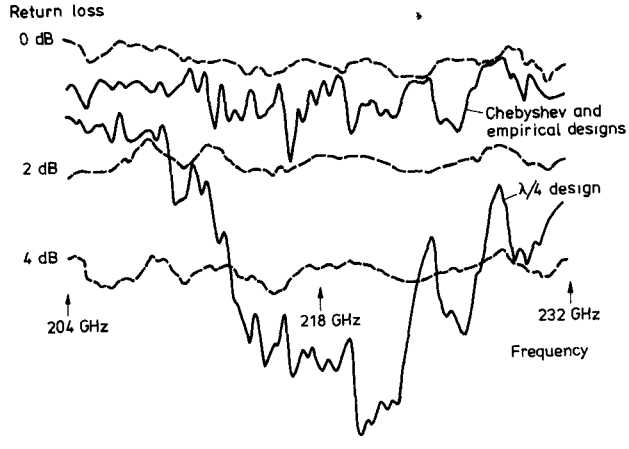

Fig. 7. Experimental return loss at second harmonic frequencies.

directivity were used to measure the reflected power. The detected signals were fed onto a scalar network analyzer which subtracted the reference signal from the test signal. In this way, the effects of unequal signal power and detector response versus frequency were minimized.

C. Experimental Results

In the 75–116-GHz frequency band, return losses of 1.0–0.8 dB were measured, respectively, for the Chebyshev-derived and empirical designs. For the $\lambda/4$ design, the return loss was slightly higher at around 90 GHz. The resulting VSWR was between 60 and 90 (+100 percent, −10 percent) for the Chebyshev-derived and empirical designs. The $\lambda/4$ design resulted in a VSWR of between 30 and 90 for this frequency region.

Fig. 7 shows typical results for the second harmonic band. Only one curve represents the results for the Chebyshev-derived and empirical designs as the results were indistinguishable over the region tested. The VSWR for these shorts is approximately the same as that measured at the fundamental frequencies. The $\lambda/4$ design, on the other hand, show marked degradation in performance as expected. VSWR's of only 4–20 were measured for it at second harmonic frequencies.

In the tests reported here, 3 to 5 samples of each type of

design were used. The machining tolerance for the section lengths was ± 25 μm. The performance of each backshort design was repeatable from short to short to high accuracy.

The same shorts were also tested before they were copper plated. Return losses of 0.1–0.3 dB higher were measured in every case in both the 75–116-GHz and 204–232-GHz frequency bands.

V. Conclusions

The goal of this study has been to develop noncontacting backshort designs which will maintain a high VSWR throughout both the full frequency band of WR-10 waveguide and its second harmonic. It has not been found possible to create a design that would cover this entire range without gaps. It has, however, been found possible, having started with an optimum Chebyshev design, to create, through the judicious use of scaling and adjustment of individual element lengths, an acceptable backshort design. Thus, it is apparent that low-frequency filter design techniques can be helpful in designing and optimizing noncontacting backshorts for use at millimeter-wave frequencies. This design seems to be quite generally applicable in that it has been scaled with success for use in both WR-8 and WR-15 reduced height waveguide. An empirical backshort design has also been created with success.

These designs have been extensively tested at both fundamental and second harmonic frequencies. To the knowledge of the authors, this has been the first experimental work to have used swept frequency techniques at frequencies above 200 GHz.

One consideration that has been ignored throughout this work is the effect of higher order traveling wave modes on the design. These modes could be quite important at second harmonic frequencies. They could also be of some importance at fundamental frequencies as it is found that the dielectric loaded low-impedance sections of the shorts overmode at quite low frequencies [5]. In the case of the shorts designed here, these sections overmode at 67 GHz. This is even below the lower end of the fundamental band in WR-10 guide. The fact that these shorts work well, however, seems to indicate that this overmoding is not important.

References

[1] A. V. Räisänen and M. K. Brewer, "Design and test of wideband noncontacting millimeter waveguide backshorts," in *Proc. Fifth Int. Conf. on Infrared and Millimeter Waves*, (Würzburg, West Germany), Oct. 1980, pp. 113–114.

[2] A. V. Räisänen, C. R. Predmore, P. T. Parrish, P. F. Goldsmith, J. L. Marrero, R. A. Kot, and M. V. Schneider, "A cooled schottky diode mixer for 75–120 GHz," in *Proc. 10th European Microwave Conf.*, (Warsaw, Poland) Sept. 1980.

[3] G. L. Matthaei, L. Young, and E. M. T. Jones, *Design of Microwave Filters, Impedance Matching Networks, and Coupling Structures*, vol. 1. New York: McGraw-Hill, 1964, pp. 95–104 and pp. 361–369.

[4] R. F. Harrington, *Time-Harmonic Electromagnetic Fields*. New York: McGraw-Hill, 1961, pp. 158–161.

[5] F. E. Gardiol and A. S. Vander Vorst, "Wave propagation in a rectangular waveguide loaded with an *H*-plane dielectric slab," *IEEE Trans. Microwave Theory Tech.*, vol. MTT-17, pp. 56–57, Jan. 1969.

[6] N. Marcuvitz, Ed., *Waveguide Handbook* New York: McGraw-Hill, 1951, pp. 307–310.

[7] J. R. Warner, *DIGRAPH User's Guide*. Boulder: Univ. Colorado Press, 1979.

[8] F. J. Tischer, "Experimental attenuation of rectangular waveguides at millimeter wavelengths," *IEEE Trans. Microwave Theory Tech.*, vol. MTT-27, pp. 31–37, Jan. 1979.

[9] R. W. Haas and B. Vowinkel, "Low frequency modeling of coaxial low pass filters for use in millimeter wavelength mixers," Tech. Rep. 46, Max Planck Institute for Radioastronomy, Bonn, West Germany.

[10] N. R. Erickson, "A 200–300-GHz heterodyne receiver," in *Proc. IEEE MTT-S Int. Microwave Symp.*, (Washington D. C.), 1980.

Michael K. Brewer was born in Seattle, WA., on Sept. 20, 1948. He received the B.S. degree in physics from the University of Washington, Seattle, in 1975. From 1975 to the present he has been engaged as a graduate research assistant at the University of Massachusetts, Amherst, where he is currently writing his doctoral dissertation in the field of radio astronomy. His interests include both receiver development and molecular cloud physics.

Antti V. Räisänen was born in Pielavesi, Finland, on Sept. 3, 1950. He received the Diploma Engineer (M.Sc.), the Licentiate of Technology, and the Doctor of Technology degrees in electrical engineering from the Helsinki University of Technology, Helinski, Finland, in 1973, 1976, and 1981, respectively.

From 1974 to 1978 he worked as a research assistant at the Helsinki University of Technology (HUT) Radio Laboratory. From 1978 to 1979 he was a research assistant at the Five College Radio Astronomy Observatory (FCRAO) at the University of Massachusetts, in Amherst. Since 1980 he has been a research fellow of the Academy of Finland, working both at HUT and FCRAO. His current research interest is the development of low-noise mixers and other components for millimeter wave receivers.

Dr. Räisänen is the Secretary of the European Microwave Conference 1982.